19. The differential Doppler shift F_D of a signal received on Earth after scattering by a ring particle is measured with respect to the directly propagating signal. Loci of constant F_D form contours of constant Doppler shift in the ring plane. The Voyager 1 trajectory was chosen to align these Doppler contours with coordinates of constant radius within the ring plane to the extent possible. An osculating condition between the Doppler contours and the azimuthal ring coordinate was achieved within the area illuminated by the spacecraft antenna, so there is a strong mapping between the Doppler shift of the received signals and radial ring position (*1*).
20. Integration times were changed in the course of the experiment from about 6 to about 3 seconds; precise values are not available for this system. The standard deviation of a single smoothed spectrum is estimated to be slightly greater than 0.5 dB or 10 percent, which is consistent with the other parameters of the system.
21. The nominal value of the optical depth of the B ring, estimated from previous Earth-based observations, is in the range 1 to 1.5 measured perpendicular to the ring plane. At Voyager 1 encounter the obliquity of the ring plane relative to the Voyager-Earth line was 6.1°, so that the effective optical depth along the ray path is about one order of magnitude greater than the normal optical depth. Consequently, the estimated attenuation along the radio path is in the range 40 to 60 dB, assuming the ring particles are all large with respect to the microwave wavelengths employed. Processing of the data recordings from the tracking station (*4*) should permit detection and measurement of the direct signal attenuation in this range.
22. E. A. Marouf, thesis, Stanford University, Stanford, Calif. (1975).
23. Optical depth is obtained directly from the reduction in direct signal intensity measured in spectra from the real-time monitoring system. The values given represent averages over radial extents of several hundred kilometers in the ring plane. Particle scattering gain is calculated from the intensity of the forward-scattered radiation relative to the noise and the known parameters of the signal path. This gain is relative to a slab of isotropic scatterers of the same optical depth. E. A. Marouf has calculated parametric curves for the exact forward-scattering cross section as a function of optical depth over a range of monodispersive size distributions. These curves are appropriate to the Voyager geometry and include multiple scatter. For the monodispersive case, the optical depth and scattering cross-section yield a unique solution for particle size. Marouf assumed a cloudlike distribution of particles surrounding the mean ring plane. If future results indicate that the particles lie essentially in a monolayer, the particle sizes must be recalculated.
24. Forward scattering from the outer third of the Cassini division is approximately 6 dB stronger than that from the adjacent inner portion of the Cassini division or the A ring. Variations in the strength of this feature as the direct ray approached and then passed through the Cassini division can be mapped to yield the forward-scattering phase function of particles. The half-power width of the scattering lobe is approximately 0.25° at 3.6 cm, implying a particle size for a monodispersive distribution of about 8 m.
25. H. Alfvén and G. Arrhenius, *NASA Spec. Publ. SP-345* (1976).
26. J. N. Cuzzi and J. B. Pollack, *Icarus* **33**, 233 (1978); E. E. Epstein, M. A. Janssen, J. N. Cuzzi, W. G. Fogarty, J. Mottmann, *ibid.* **41**, 103 (1980). J. N. Cuzzi, J. B. Pollack, A. L. Summers, manuscript "Saturn's rings: Particle composition and size distribution as constrained by observations at microwave wavelengths II," Radio Interferometric Observations (1980).
27. H. Jeffreys (*28*) gives a value for the mass of Rhea of $3.2 \pm 3.8 \times 10^{-6}$ M_S, Y. Kozai (*29*) gives $9.0 \pm 2.6 \times 10^{-6}$ M_S, and W. I. McLaughlin and T. D. Talbot [*Mon. Not. R. Astron. Soc.* **179**, 619 (1977)] give $4.8 \pm 0.8 \times 10^{-6}$ M_S; all are based on orbital precessions in the Saturn satellite system. J. D. Anderson *et al.* (*30*) give $3.8 \pm 1.3 \times 10^{-6}$ M_S, and G. W. Null *et al.* (*31*) give $4.0 \pm 0.9 \times 10^{-6}$ M_S, both from the Pioneer 11 flyby.
28. H. Jeffreys, *Mon. Not. R. Astron. Soc.* **114**, 433 (1954).
29. Y. Kozai, *Publ. Astron. Soc. Jpn.* **28**, 675 (1976).
30. J. D. Anderson, G. W. Null, E. D. Biller, S. K. Wong, W. B. Hubbard, J. J. MacFarlane, *Science* **207**, 449 (1980).
31. G. W. Null, E. L. Lau, E. D. Biller, J. D. Anderson, *Astron. J.*, in press.
32. W. S. Eichelberger [*Publ. U.S. Nav. Obs. 6* (1911), appendix 2B, p. 1] gives $239.7 \pm 4.9 \times 10^{-6}$ M_S for the mass of Titan from a numerical integration of the orbit of Hyperion. H. Jeffreys (*28*) gives $241.2 \pm 1.8 \times 10^{-6}$ M_S from perturbations on Iapetus; J. D. Anderson *et al.* (*30*) give $237.0 \pm 2.7 \times 10^{-6}$ M_S from the Pioneer flyby; G. W. Null *et al.* (*31*) give $238.8 \pm 3.0 \times 10^{-6}$ M_S from a combined analysis of Pioneer 11 and satellite dynamics data. P. J. Message [*Trans. Int. Astron. Union* **10**, 111 (1958)] gives a high value of $246.22 \pm 0.13 \times 10^{-6}$ M_S from perturbations on Hyperion. However, Message later [in *Dynamics of the Solar System*, R. L. Duncombe, Ed. (Reidel, Dordrecht, Netherlands, 1979), p. 159] discussed errors in the satellite theory for Hyperion and difficulties in deriving a mass for Titan from the theory. The numerical integration of Eichelberger avoids these difficulties.
33. G. W. Null, *Astron. J.* **81**, 1153 (1976).
34. M. E. Davies, T. A. Hauge, F. Y. Katayama, J. A. Roth, *Rand Corp. Rep. R-2532-JPL/NASA* (1979).
35. M. J. Lupo and J. S. Lewis, *Icarus* **40**, 157 (1979).

36. We thank the members of the Voyager Project operations teams and the Deep Space Network for their support in acquisition of the radio science data. We thank the Voyager navigation team, in particular J. K. Campbell, R. A. Jacobson, and S. P. Synnott, for making available their preliminary fits to the two-way Doppler and optical navigation data and the Voyager imaging team for prepublication values of radii. We also thank A. J. R. Prentice for numerous discussions and assistance in the interpretation of the mean densities of the satellites of Saturn. We especially thank B. J. Buckles, P. E. Doms, D. F. Finnerty, and D. P. Holmes for their efforts in the implementation and execution of these experiments and H. B. Hotz and D. N. Sweetnam for their help in the profile computation. E. A. Marouf has played a vital role over many years in the concept, development, design, implementation, and analysis of the ring occultation experiment and we gratefully acknowledge his contribution. This work was supported by the National Aeronautics and Space Administration.

9 February 1981

Extreme Ultraviolet Observations from Voyager 1 Encounter with Saturn

Abstract. *The global hydrogen Lyman α, helium (584 angstroms), and molecular hydrogen band emissions from Saturn are qualitatively similar to those of Jupiter, but the Saturn observations emphasize that the H_2 band excitation mechanism is closely related to the solar flux. Auroras occur near 80° latitude, suggesting Earth-like magnetotail activity, quite different from the dominant Io plasma torus mechanism at Jupiter. No ion emissions have been detected from the magnetosphere of Saturn, but the rings have a hydrogen atmosphere; atomic hydrogen is also present in a torus between 8 and 25 Saturn radii. Nitrogen emission excited by particles has been detected in the Titan dayglow and bright limb scans. Enhancement of the nitrogen emission is observed in the region of interaction between Titan's atmosphere and the corotating plasma in Saturn's plasmasphere. No particle-excited emission has been detected from the dark atmosphere of Titan. The absorption profile of the atmosphere determined by the solar occultation experiment, combined with constraints from the dayglow observations and temperature information, indicate that N_2 is the dominant species. A double layer structure has been detected above Titan's limb. One of the layers may be related to visible layers in the images of Titan.*

Saturn's atmosphere. Saturn's upper atmosphere is qualitatively similar to Jupiter's, consisting mainly of H, H_2, and He above a layer of ultraviolet (UV)-absorbing hydrocarbons. These constituents are measured in emission and absorption by the Voyager ultraviolet spectrometer (UVS) (*1*).

Hydrogen Lyman α (Ly α) emission arises from resonance scattering of the solar line at 1216 Å and by particle excitation. The disk-averaged Ly α brightness of Saturn measured from rocket and Earth-orbital experiments ranges from 0.7 kR (kilorayleigh) (*2, 3*) to 1.5 kR (*4*). The Voyager UVS found a central-disk brightness of 3.3 kR, which corresponds to a disk-averaged brightness of 1.5 kR if the brightness varies as a cosine function from center to limb. A few hundreds of rayleighs of this emission may arise in the H atmosphere of the rings. The implied H column abundance on Saturn is about 5×10^{16} cm^{-2}, somewhat less than the abundance of 1×10^{17} to 3×10^{17} cm^{-2} at Jupiter (*1*). Helium (584 Å) emission is scattered from the strong solar line at that wavelength. The measured central-disk intensity is 2.2 ± 0.3 R, but a substantial part of this may arise in the extended region out to 25 Saturn radii (R_S).

As at Jupiter, the Lyman and Werner bands of H_2 are also radiated from the dayside disk. Figure 1 compares spectra from the central regions of Saturn and Jupiter taken under similar conditions. The intensity integrated over the H_2 Lyman and Werner bands is about 0.7 kR, or about 25 percent of the intensity at Jupiter. This factor of 4 is nearly the same as the factor of 3.3 reduction in solar flux from Jupiter to Saturn. The general structure of the Jupiter and Saturn spectra between 900 and 1700 Å is similar, although there are differences between 1100 and 1200 Å and in the region near 1570 Å (Fig. 1).

Emissions from the dark atmosphere of Saturn at Ly α (0.35 kR) and He (584

0036-8075/81/0410-0206$01.00/0

Å) (0.4 ± 0.2 R) were detected from equatorial and mid-latitudes. The Ly α radiation can probably be excited by resonance scattering of the sky background Ly α by atmospheric H as at Jupiter (*5*), although there may be a substantial contribution to the observed Ly α from the sunlit portion of the ring atmosphere in the field of view. As at Jupiter, no H_2 band emission has been detected from the nightside, except in the polar aurora discussed later. The current upper limit of about 10 R is a factor of 70 less than the emission on the dayside.

First efforts to understand the equatorial H_2 band emission from Jupiter relied on H_2 excitation by precipitating magnetospheric electrons (*1, 6*). This source was not entirely satisfactory because it did not offer an explanation for the observed day-to-night difference in H_2 band intensity, a factor of at least 10. Several facts now suggest that the H_2 bands from Saturn and Jupiter are excited by a source stimulated by solar radiation: (i) The intensities of the H_2 bands at Jupiter and Saturn are in almost the same ratio as the solar fluxes. In contrast, trapped particle populations at the two planets differ by much more than a factor of 4. (ii) The day-to-night brightness ratio at Saturn is at least 70, a much more stringent limit than could be determined at Jupiter. (iii) The H_2 bands are present at Saturn's equator and mid-latitudes, whereas no significant direct particle precipitation into the atmosphere is expected between the equator and the *L* shell of the outer edge of the rings, which reaches the atmosphere at about 50° latitude. (iv) The H_2 band intensity within the shadow of the rings is less than on the unshadowed planet.

On the basis of solar extreme ultraviolet emission rates obtained in December 1979 (*7*), solar radiation deposits 2×10^{-2} erg cm^{-2} sec^{-1} in photoelectron energy. An improbably large efficiency of 65 percent in the conversion of photoelectron energy to H_2 band radiation is required if the 1.3×10^{-2} erg cm^{-2} sec^{-1} radiated in the H_2 bands is to be supplied by the solar flux alone. Therefore an additional energy source is needed.

Aurora. Prior to the Voyager encounter at Saturn, observations made with the International Ultraviolet Explorer satellite (*3*) and the ultraviolet photometer aboard Pioneer 11 (*8*) suggested the presence of auroras on Saturn, but both observations were ambiguous. The UVS measured clearly defined auroras, consisting of Ly α and H_2 Lyman and Werner band emissions, from the polar regions of both hemispheres. A scan from mid-latitudes across the south pole showed auroral emission between 78°S and 81.5°S at $\lambda_{SLS} = 190$. Within the polar cap region no auroral emission was detected. The intensity in the H_2 bands was 2 to 3 kR. The position of the aurora corresponds fairly well to the edge of the polar cap inferred from the Voyager magnetic field measurements (*9*).

During the post-encounter north-south map (NSM) sequence (*10*), the average brightness of the northern aurora was 10 to 15 kR in the H_2 bands and about 10 kR in Ly α (see Table 1). These values depend on the measured apparent brightness and the fraction of the field filled by the emission, which was estimated from the south polar scan. During both pre- and post-encounter NSM's, the brightness of the aurora changed by factors of 3 to 4 within 3 hours. In both maps, the brightest regions were at $0° < \lambda_{SLS} < 120°$, roughly the longitude of the pre-encounter peak in radio emission (*11*). For an assumed average brightness of 5 kR in the H_2 bands, and an auroral zone bounded by 78° and 81.5° latitude in both hemispheres, about 2×10^{11} W must be deposited in the atmosphere by precipitating electrons.

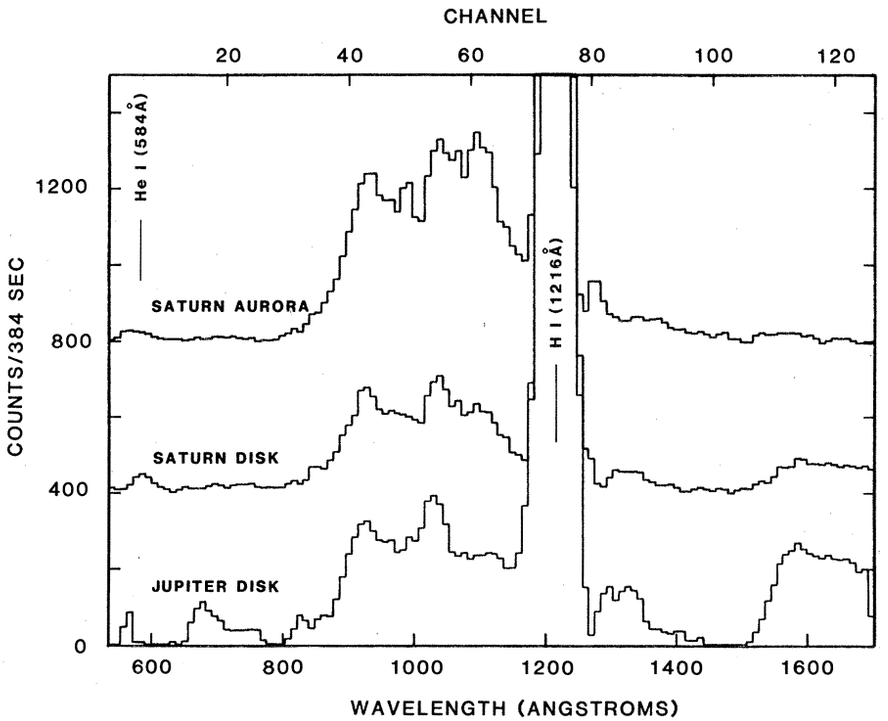

Fig. 1. Planetary spectra showing emission at H Ly α, He 584 Å, and in the Lyman and Werner bands of H_2 (900 to 1130 Å). The spectra labeled Jupiter and Saturn are from the central region of the disk. The Jupiter spectrum contains emission from the plasma torus in the wavelength range 670 to 800 Å. The Saturn spectrum has been multiplied by 3.3, the ratio of the solar flux at Jupiter to that at Saturn. Comparison with the Jupiter spectrum shows that the intensity of the H_2 bands approximately follows the solar flux at the two planets. The auroral spectrum is enhanced in both H and H_2 emissions. The relatively brighter H_2 band feature at 1106 Å indicates self-absorption in a deep H_2 column.

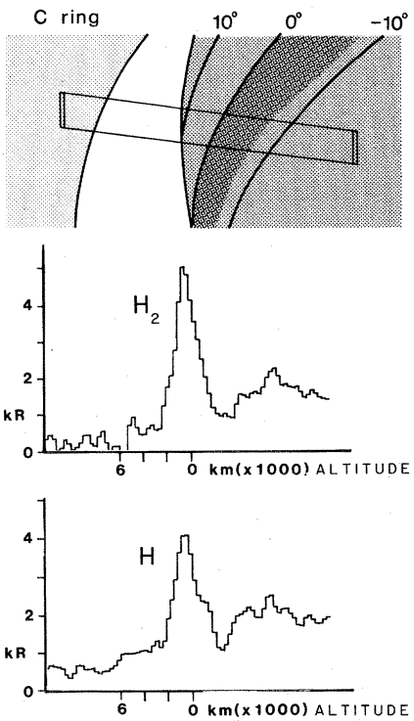

Fig. 2. Saturn limb drift, showing Ly α and H_2 emission profiles off the bright limb and onto the disk of Saturn. The position of the visible limb was determined from support imaging frames. The drop in brightness just past the limb corresponds to the shadow of the ring, which is shown as the dark band on the planet.

Table 1. Brightness of selected features in Saturn's spectrum. The data are expressed in rayleighs.

Location	H Ly α	He (584 Å)	H_2 bands
Dayside	3300*	2.2*	700
Nightside	350*	0.4*	< 10
Aurora	10^3 to 2×10^4		2×10^3 to 2×10^4

*May include a substantial contribution from the ring atmosphere or magnetosphere.

Drifts across the bright limb of Saturn (Fig. 2) show that both Ly α and H_2 band emissions have strong peaks about 800 km above the limb. Self-absorption characteristics of the spectra imply that the auroral source is lower in altitude than the low-latitude H_2 emissions, and this is consistent with the fact that the H_2 band spectra from the central disk and from the equatorial limb are similar in spite of large path length differences, indicating optically thin conditions in both cases.

The UVS observed the solar spectrum as the sun set behind the planet and measured extinction by the atmosphere as a function of altitude and wavelength. Analysis of the transmission near 600 Å shows a scale height of 400 ± 50 km. If H_2 is the dominant absorber at this wavelength, the temperature is 850 ± 100 K and the concentration of H_2 is 1.2×10^8 cm^{-3} at r = 62,650 km from Saturn's center. The H absorption region near 900 Å shows a scale height of 750 ± 100 km, corresponding to a temperature of 820 ± 100 K, in good agreement with that inferred from H_2 absorption. The density of [H] = 1×10^8 cm^{-3} at r = 61,600 km. The occultation occurred at 30° latitude where the visible limb has a radius of 58,700 km. The neutral temperature measured in the equatorial exosphere by the UVS is therefore virtually the same as the plasma temperature inferred at 79°S (*12*).

Rings. Resonance-scattered Ly α emission was detected from neutral hydrogen gas associated with Saturn's rings. No other emissions have been detected in the examined data sets. Upper limits for several strong oxygen lines that are reasonable candidates for excitation in any electrical discharge type phenomena (*11*) associated with the rings are O I (989 Å), O II (834 Å), O III (703, 834 Å) < 0.6 *R*, and O I (1304 Å) < 2.6 R.

A scan across the rings (Fig. 3) shows a highly variable Ly α signal from the sky background transmitted by the rings and a neutral hydrogen ring atmosphere. Contamination by the sky background can be avoided by using observations of the B ring taken at grazing aspect so that the effective optical depth is greater than 3 (*13, 14*). The Ly α albedo of the B ring does not contribute significantly; the B ring's sunlit and dark sides have almost identical brightnesses. Thus the Ly α brightness of 360 R measured under these conditions must be resonance-scattered by H atoms between the spacecraft and the rings.

The limb drift observations show no Ly α emission (over the level of the sky background plus torus) far above the limb of Saturn, so this hydrogen probably comes from the ring particles. If the hydrogen is distributed in a torus having a circular cross section of radius 1 R_S, then an H column density of 1×10^{13} cm is required for optically thin conditions. For a uniformly distributed cloud, the number density is 600 cm^{-3} and the content of the cloud is about 5×10^{33} atoms.

This density is similar to previous measurements. A density of 400 cm^{-3} was derived by interpretation (*15*) of a rocket observation (*2*). This large amount of hydrogen is difficult to explain by proposed source mechanisms (*16, 17*), suggesting that it may be necessary to reexamine the H loss mechanisms, in particular the sticking coefficients for H on H_2O ice.

At present the Ly α signature of the rings is difficult to reconcile with the Pioneer 11 ultraviolet photometer observations (*8*). This is probably due in part to the different nature of the instruments, the observational techniques, and the

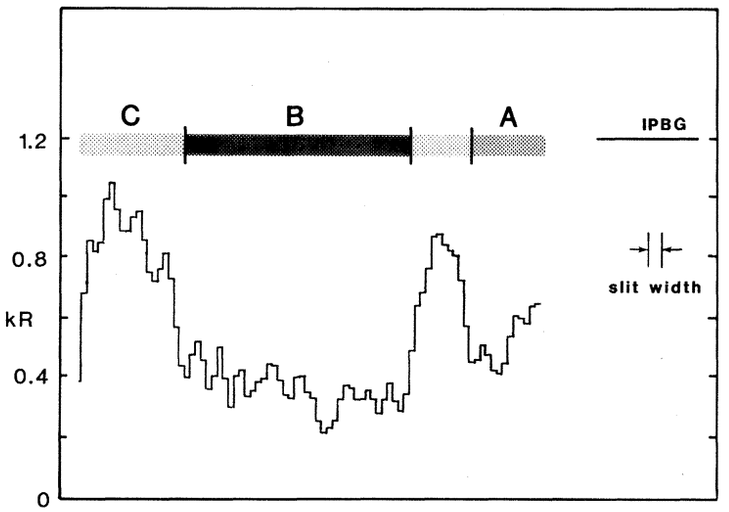

Fig. 3 (above). Brightness of Ly α across the illuminated side of the rings. The rings were scanned from the middle of the C ring to the middle of the A ring. The signal increase between the B and A rings is due to transmission of the sky background by Cassini's division. The UVS slit was oriented approximately perpendicular to the radial dimension of the rings with an average slit width of 0.1 R_S.

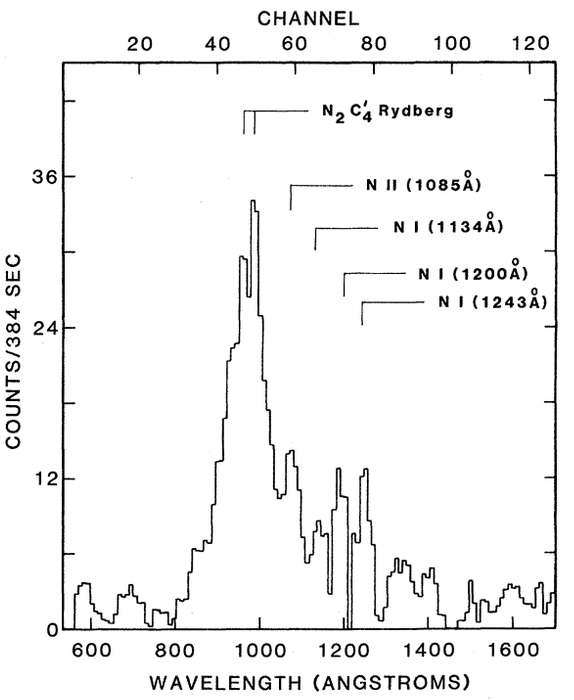

Fig. 4 (right). The disk-averaged spectrum of Titan's dayglow. A synthetic Ly α line has been subtracted to show lines at about 1200 Å and about 1240 Å. Many of the features correspond to electron-excited nitrogen. No other species have been identified but upper limits have been placed on plausible extreme ultraviolet emitters (Table 2). Many of the features longward of 1250 Å may be N_2 LBH bands.

viewing geometry provided by the different trajectories.

Titan. Except for the presence of CH_4, little was known of the composition and depth of Titan's atmosphere before the Voyager 1 encounter with Saturn. Models of the formation of Titan (*18*) led to the argument by Hunten (*19*) that the dominant atmospheric gas may be N_2. The atmospheric evolution models of Atreya *et al.* (*20*) have shown that a thick atmosphere of N_2 can be formed on Titan by photolysis of the outgassed NH_3. The combined Voyager experiments of radio science (*12*), infrared spectroscopy (IRIS) (*21*), and extreme ultraviolet spectrometry now indicate that N_2 is indeed the dominant atmospheric gas.

Titan's dayside airglow spectrum (Fig. 4) is similar to laboratory spectra of electron-excited N_2 (*22*), with the inclusion of a strong Ly α line. The Ly α line is the only emission detected so far in the dark atmosphere. The peaks at 960 Å and 980 Å correspond to the strong Rydberg ($c'_4\ ^1\Sigma_u^+ - X^1\Sigma_g^+$) (0,0) and (0,1) bands. The transitions arising in the c'_4 state account for about 60 percent of all extreme ultraviolet N_2 band emission under optically thin conditions (*23*). The relative intensities of the bands suggest a column density of about 10^{15} cm^{-2} (*24*).

Table 2. Titan data.

Species	Observed intensity (R)	Predicted intensity (R)
N_2 ($c'_4\ ^1\Sigma_u^+ - X^1\Sigma_g^+$) (0,0)	10	
and (0,1)	12	
N_2 Σ (800 Å to 1020 Å)	43	
N II (1085 Å)	7	6.0*
N I (1135 Å)	5	2.5* 14.0†
N I (1200 Å)	18	14.0* 18.0†
N I (1243 Å)	25	3.3* 0.4†
H I (1216 Å)	500	
Ne I (736 Å)	< 0.15	
A I (1048 Å)	< 4	
H_2 (Lyman and Werner)	< 35	
N_2 LBH (1383 Å)	< 10	2‡ + 5§ = 7
	Density ratios	
[Ne I]/[N_2]	$< 1 \times 10^{-2}$	R = 4000 km
[A I]/[N_2]	$< 6 \times 10^{-2}$	[N_2] = 10^8 cm^{-3}
[H_2]/[N_2]	< 0.2	

*Based on e + N_2 relative to N_2 Rydberg bands in optically thin gas (1.5×10^9 W input). †e + N I, optically thin relative values normalized to N I (1200 Å). ‡e + N_2 at 4000 km relative to N_2 Rydberg bands. §e + N_2 due to photoelectrons (10^9 W input) at 3600 km. See text.

The bright limb scans (Fig. 5) show that the N_2 band emission occurs at 3600 km from planet center on the side facing into the corotating magnetospheric plasma. The occultation experiment discussed below indicates a vertical abundance of 5×10^{16} cm^{-2} above 3600 km. This suggests that the limb-brightened peak in N_2 emission is about 400 km lower than the source of the spectrum in Fig. 4. The limb spectrum, not shown here, has the appearance of an optically thick source.

The predicted and measured relative intensities shown in Table 2 suggest that the excitation of N I and N II multiplets is dominated by the e + N_2 process (*25–27*) rather than e + N. The peak in the spectrum at an apparent location of 1075 Å is interpreted as the N II (1085 Å) line,

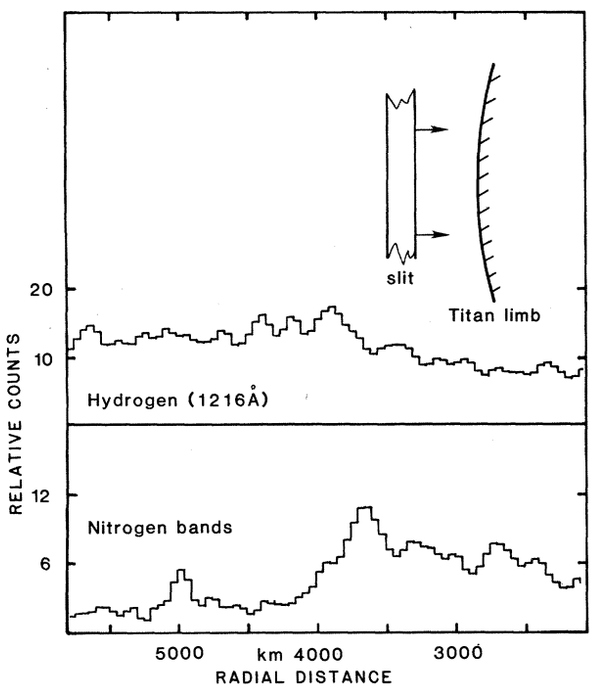

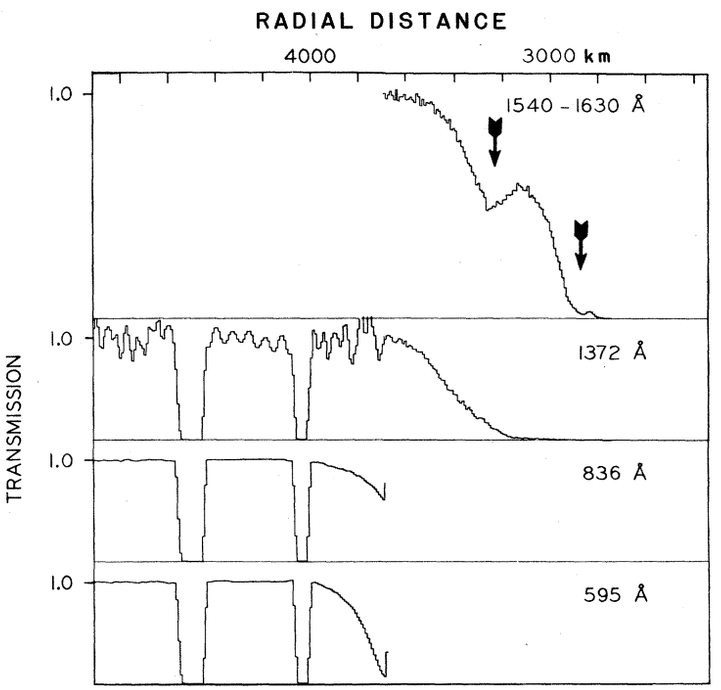

Fig. 5 (left). Ly α and N_2 Rydberg band emission as a function of altitude. High above the limb the Ly α emission of about 1 kR is attributed to the sky background and the H torus. The Ly α peak at 3900 km above the center of the planet is attributed to H in Titan's atmosphere. The emission declines to 500 R when the slit is filled by the sunlit disk. N_2 emission is not detectable above 4500 km. The narrow feature at 5000 km is not due to N_2 bands; the emitter has not been identified. Fig. 6. Transmission plotted against altitude for several wavelengths during the occultation of the sun by Titan. A change in the gain of the electron multiplier at the discontinuity at 3350 km greatly extended the altitude range of the observation. Absorption at 595 Å is attributed to N_2. The features marked by arrows in the top panel indicate a two-layer structure as discussed in the text. A change in transmission rate of the spacecraft data caused the data dropouts at 4000 km and 4250 km. The periodic structure between the dropouts in the 1372-Å curve is an artifact of the data reduction procedure and the reduced time resolution.

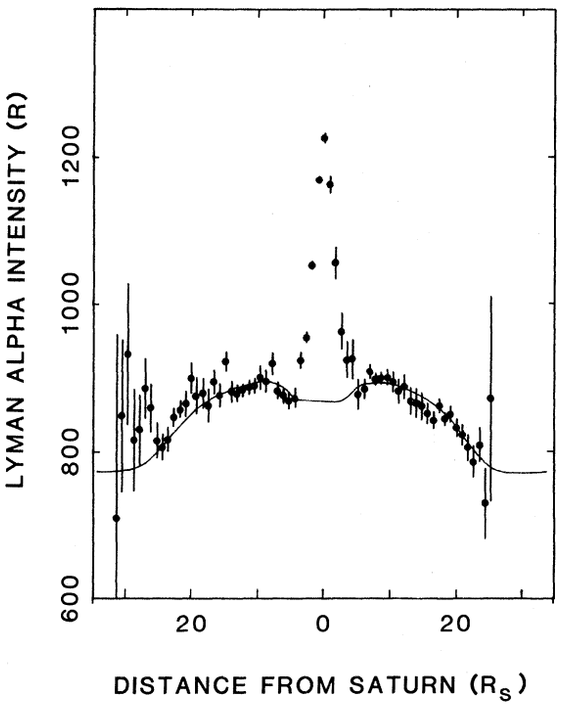

Fig. 7. The neutral hydrogen torus. The data points show the Ly α intensity as a function of distance from Saturn in the equatorial plane. The Ly α sky background is about 800 R. The error bars show ± 1 standard deviation implied by counting statistics. The central spike comes from Saturn itself. Wings extending to about 25 R_S are produced by resonance scattering of sunlight by hydrogen surrounding Saturn. The solid line shows the intensity profile that would be produced by an annular cloud of uniform hydrogen density extending from about 8 R_S to about 25 R_S near the equatorial plane. In this model, no hydrogen is present inside 8 R_S, and optically thin conditions are assumed.

which cannot be efficiently excited by photoelectrons. The intensity of the N_2 dayglow is about 40 R which, on the basis of electron excitation and an ionization efficiency of 2.8×10^{-2} ion pairs per electron volt, implies an energy deposition rate of $\sim 2 \times 10^9$ W.

The nitrogen excitation depends on solar radiation at least as a catalyst, because particle excitation is not measurable in the dark atmosphere. Since the depth of the N_2 Rydberg band emission source is too low at the bright limb, and too high on the subsolar side, to be accounted for by photoelectrons alone, we require the introduction of additional processes. This interpretation suggests current sheet excitation resulting from the interaction of Saturn's magnetosphere with the ionosphere, leading to the production of > 0.1 keV electrons at high altitudes.

The aeronomical consequences of the observed N_2 emission are important beyond the fact that N_2 is present in Titan's atmosphere. Electron impact on N_2 leads to dissociation of N_2 into fragments composed of $N(^2D) + N(^4S)$ (*28, 29*), and $N^+ + N$. About 40 percent of these N atoms produced in the exosphere will escape (*30*). Nearly all the remaining N_2 fragments react with hydrocarbons to produce HCN which accumulates in the thermal inversion layer in concentrations (*30*) observable by the Voyager IRIS experiment (*21*).

Figure 5 shows the altitude profile of the Ly α emission. The decline in intensity toward the limb from the peak is due to absorption of the sky background by the atmosphere. The Ly α intensity is about 0.5 kR on the dayside and about 0.3 kR on the nightside. A preliminary analysis of these data indicates an atomic hydrogen density of $\sim 4 \times 10^4$ cm^{-3} at 4000 km, compared to 10^8 cm^{-3} for N_2. An upper limit on the intensity of H_2 Lyman and Werner bands leads to an estimate $[H_2]/[N_2] \leq 0.2$ (Table 2) at 4000 km. Using a measured cross section (*31*) for A I (1048 Å) and a theoretical estimate (*32*) for Ne I (736 Å) of 3.9×10^{-17} cm^{-2} and 1.0×10^{-17} cm^{-2}, respectively, we obtain the upper limits $[A\ I]/[N_2] \leq 6 \times 10^{-2}$ and $[Ne\ I]/[N_2] \leq 1 \times 10^{-2}$. The emission features longward of 1250 Å show a rough correspondence to the Lyman-Birge-Hopfield (LBH) bands of N_2.

Both entrance and exit solar occultations by Titan's atmosphere were observed. In Fig. 6, transmission is plotted against altitude at several wavelengths from the entrance occultation experiment. The 595-Å curve indicates a scale height of 80 ± 10 km. If one considers N_2 to be the major absorber, one obtains a temperature of 165 ± 20 K at r = 3840 km from Titan's center, where $[N_2] = 2.9 \times 10^8$ cm^{-3}. Channels near Ly α probe deeper in the atmosphere, where the scale height is about 72 km. If absorption near Ly α is due primarily to CH_4, then $[CH_4] = 4.8 \times 10^8$ cm^{-3} at r = 3600 km, and the temperature is 170 K, assuming a mixed atmosphere at this level.

Extrapolation of the N_2 density measured at 3840 km down to 3600 km yields a pressure of 1.7×10^{-7} mbar.

The transmission curve shown in the top panel of Fig. 6 shows evidence for layers at about 3335 and 2965 km from the center of Titan. The thickness of each of the layers is 70 ± 20 km. The lower layer is located near one of the "haze layers" in the visible images, but no visible feature corresponding to the upper layer has been identified (*33*).

The absence of a signature from the upper layer in the 1372-Å curve of Fig. 6, taken with the strong signature at 1540 to 1630 Å, constrains the composition of the layer. It seems unlikely that absorption or scattering by dust or aerosols would vary so strongly with wavelength. A search for a molecular constituent having the proper absorption characteristics is in progress.

The hydrogen torus. The concept of a cloud of neutral hydrogen surrounding Saturn near the orbit of Titan was first proposed by McDonough and Brice in 1973 (*34*). Hydrogen atoms and molecules, the eventual product of photolysis of methane in Titan's atmosphere, can easily escape from Titan because of the weak gravitational field of the satellite. This gas, bound by Saturn's gravity, forms a torus-like cloud centered on Saturn. Neutral hydrogen in Saturn's system has been detected or suggested (*2, 4, 8*), but little information about its distribution has been available until the Voyager flyby.

Figure 7 shows the Ly α intensity profile measured by the UVS. These data were accumulated over 14 days, nearly one orbital period of Titan. The absence of peaks near the elongation points of Titan's orbit means that the hydrogen must be distributed widely in the system, not confined closely to the orbit. The solid curve in Fig. 7 shows the profile that would result from a cloud of uniform density encircling Saturn between 8 and 25 R_S, near the equatorial plane. Most of the hydrogen is confined to within 6 R_S, and possibly closer, to the equatorial plane. If the cloud height is greater than 6 R_S (3 R_S above and below the plane), the UVS slit is filled and the hydrogen density is 10 cm^{-3} based on the model path length, the peak brightness of about 100 R, and the assumption of an optically thin medium. A height of 6 R_S implies a cloud volume of 2×10^{33} cm. The content would then be 2×10^{34} H atoms, nearly the same as the model results of Smyth (*35*). If the lifetime of a neutral H atom is 10^7 seconds (*8*) then the required supply rate is 2×10^{27} atoms per second. If the hydrogen comes from Titan, a source of 2×10^9 atoms cm^{-2} sec^{-1} at a radius of 3000 km is required.

Photolysis of the CH_4 observed in Titan's atmosphere should give a predictable source of H_2; this was estimated by Hunten (*19*) from the photochemical results of Strobel (*36*). It is 9×10^9 cm^{-2} sec^{-1}, referred to a radius of approximately 3000 km. The total escape rate is therefore $E(H_2) = 3.4 \times 10^{27}$ sec^{-1}.

The source of the H actually observed in the torus is probably less than the H_2 source. Strobel (*36*) included an "ionospheric source" of 10^8 H atoms cm^{-2} sec^{-1}, most of which probably would escape. The model predicts an escape rate of 6×10^8 cm^{-2} sec^{-1} from methane photolysis. We should also examine the ionospheric source. At the subsolar point, N_2^+ is presumably being produced at a column rate of 4×10^8 cm^{-2} sec^{-1}. It reacts with H_2 by

$$N_2^+ + H_2 \rightarrow N_2H^+ + H \quad (1)$$

$$N_2H^+ + e \rightarrow N_2 + H \quad (2)$$

to produce two H atoms for each N_2^+.

Most of the H atoms will escape thermally. The globally averaged escape rate is $\simeq 1.4 \times 10^{27}$ sec^{-1} for the ionospheric and methane sources (*37*), just the quantity required by the torus. Additional H atoms may be supplied from ionization of H_2 in the torus region followed by

$$H_2^+ + H_2 \rightarrow H_3^+ + H \quad (3)$$

and subsequent dissociative recombination of H_3^+.

A. L. BROADFOOT, B. R. SANDEL
D. E. SHEMANSKY, J. B. HOLBERG
G. R. SMITH
Earth and Space Sciences Institute, University of Southern California, Tucson, Arizona 85713
D. F. STROBEL
Naval Research Laboratory, Washington, D.C. 20375
J. C. MCCONNELL
York University, Ontario, Canada M3J 1P3
S. KUMAR
University of Southern California, Los Angeles 90007
D. M. HUNTEN
University of Arizona, Tucson 85721
S. K. ATREYA, T. M. DONAHUE
University of Michigan, Ann Arbor 48109
H. W. MOOS
Johns Hopkins University, Baltimore, Maryland 21218
J. L. BERTAUX, J. E. BLAMONT
Service D'Aeronomie du CNRS, Verrieres le Buisson, France
R. B. POMPHREY, S. LINICK
Jet Propulsion Laboratory, Pasadena, California 91103

References and Notes

1. Details of the instrument and data analysis procedure are given by A. L. Broadfoot *et al.*, *J. Geophys. Res.*, in press.
2. H. Weiser, R. C. Vitz, H. W. Moos, *Science* **197**, 755 (1977).
3. J. T. Clarke, H. W. Moos, S. K. Atreya, A. L. Lane, *Nature (London)*, in press.
4. E. S. Barker, S. Cazes, C. Emerich, A. Vidal-Madjar, T. Owen, *Astrophys. J.*, **242**, 383 (1980).
5. J. C. McConnell, B. R. Sandel, A. L. Broadfoot, *Icarus* **43**, 128 (1980).
6. A. L. Broadfoot *et al.*, *Science* **204**, 979 (1979).
7. H. E. Hinteregger, private communication.
8. D. L. Judge, F.-M. Wu, R. W. Carlson, *Science* **207**, 431 (1980).
9. N. F. Ness, M. H. Acuña, R. P. Lepping, J. E. P. Connerney, K. W. Behannon, L. F. Burlaga, F. M. Neubauer, *Science* **212**, 211 (1981).
10. During the north-south map sequence, which covered a complete rotation of the planet, the UVS slit was scanned repeatedly from north pole to south pole as the planet rotated beneath the spacecraft.
11. J. W. Warwick *et al.*, *Science* **212**, 239 (1981).
12. G. L. Tyler, V. R. Eshleman, J. Y. Anderson, G. S. Levy, G. F. Lindal, G. E. Wood, T. A. Croft, *ibid.*, p. 201.
13. L. Froidevaux and A. P. Ingersoll, *J. Geophys. Res.* **85**, 5948 (1980).
14. T. Gehrels, *Science* **207**, 434 (1980).
15. R. W. Carlson, *Nature (London)* **283**, 461 (1980).
16. J. Blamont, in *The Rings of Saturn* (NASA SP-343, Washington, D.C., 1974).
17. M. Dennefeld, *Int. Astron. Union Symp.* **65**, 471 (1974).
18. J. S. Lewis, *Icarus* **15**, 174 (1971).
19. D. M. Hunten, in *Planetary Satellites*, J. A. Burns, Ed. (Univ. of Arizona Press, Tucson, 1977).
20. S. K. Atreya, T. M. Donahue, W. R. Kuhn, *Science* **201**, 611 (1978).
21. R. Hanel *et al.*, *ibid.* **212**, 193 (1981).
22. F. Fischer, G. Stasek, G. Schmidtke, *Geophys. Res. Lett.* **11**, 1003 (1980).
23. E. C. Zipf and R. W. McLaughlin, *Planet. Space Sci.* **26**, 449 (1978).
24. E. C. Zipf, private communication.
25. J. F. M. Aarts and F. J. DeHeer, *Physica* **52**, 45 (1971).
26. M. J. Mumma and E. C. Zipf, *J. Chem. Phys.* **55**, 5582 (1971).
27. E. J. Stone and E. C. Zipf, *ibid.* **58**, 4278 (1973).
28. H. F. Winters, *ibid.* **44**, 1472 (1966).
29. E. S. Oran, P. S. Julienne, D. F. Strobel, *J. Geophys. Res.* **80**, 3068 (1975).
30. D. F. Strobel, in preparation.
31. J. E. Mentall and H. D. Morgan, *Phys. Rev. A* **14**, 954 (1976).
32. K-H. Tan, F. G. Donaldson, J. W. McConkey, *Can. J. Phys.* **52**, 786 (1974).
33. B. A. Smith *et al.*, *Science* **212**, 163 (1981).
34. T. R. McDonough and N. M. Brice, *Icarus* **20**, 136 (1973).
35. W. A. Smyth, in preparation.
36. D. F. Strobel, *Icarus* **21**, 466 (1974).
37. F. C. Fehsenfeld, A. L. Schmeltekopf, E. E. Ferguson, *J. Chem. Phys.* **46**, 2802 (1967).
38. We thank the Voyager project personnel at JPL for the enthusiastic efforts that have made this mission a success. We thank the staff of the Earth and Space Sciences Institute, Tucson, for their untiring support. This work was supported by the JPL, California Institute of Technology, under NASA contract NAS 7-100. Additional support was provided by the Planetary Sciences Discipline of NASA's Office of Space Sciences.

9 February 1981

Magnetic Field Studies by Voyager 1: Preliminary Results at Saturn

Abstract. *Magnetic field studies by Voyager 1 have confirmed and refined certain general features of the Saturnian magnetosphere and planetary magnetic field established by Pioneer 11 in 1979. The main field of Saturn is well represented by a dipole of moment 0.21 ± 0.005 gauss-R_S^3 (where 1 Saturn radius, R_S, is 60,330 kilometers), tilted 0.7° ± 0.35° from the rotation axis and located within 0.02 R_S of the center of the planet. The radius of the magnetopause at the subsolar point was observed to be 23 R_S on the average, rather than 17 R_S. Voyager 1 discovered a magnetic tail of Saturn with a diameter of approximately 80 R_S. This tail extends away from the Sun and is similar to type II comet tails and the terrestrial and Jovian magnetic tails. Data from the very close flyby at Titan (located within the Saturnian magnetosphere) at a local time of 1330, showed an absence of any substantial intrinsic satellite magnetic field. However, the results did indicate a very well developed, induced magnetosphere with a bipolar magnetic tail. The upper limit to any possible internal satellite magnetic moment is 5 × 10^{21} gauss-cubic centimeter, equivalent to a 30-nanotesla equatorial surface field.*

The Voyager 1 magnetic field instrumentation system (*1*) operated normally throughout the Saturn encounter. This report describes preliminary results of data obtained from the multiple range, dual low-field triaxial fluxgate magnetometers mounted on the 13-m boom. For this study, vector measurements at 60-msec intervals were averaged over 1.92, 9.6, and 48 seconds, 16 minutes, and 1 hour. The ranges of the sensors were changed automatically by an onboard system so that the maximum sensitivity of ± 0.0044 nanotesla (nT), while in the lowest range of ± 8.8 nT, decreased to ± 0.513 nT in the ± 2100 nT range near closest approach.

The maximum field measured was 1093 nT, at $\theta = -40.3°$ latitude and $\phi = 184.4°$ longitude, just before closest-approach of 3.07 R_S (1 R_S = 60,330 km). It was somewhat larger than the value of 1010 nT expected on the basis of planetary magnetic field models derived from Pioneer 11 results (*2*, *3*). The axis of the magnetic dipole representing the main field of Saturn is almost aligned with the rotation axis (*2*, *3*). Thus, Voyager 1 crossed the magnetic equatorial plane only once within 20 R_S, the orbit of Titan, as the spacecraft left the Saturnian magnetosphere at a local time of 0400 and a latitude of 20° to 25°.

One of the most exciting phases of the

0036-8075/81/0410-0211$01.25/0